Summary I

- H_2 Shielding: -- $\beta(\tau)$ vs full H2, correction for sphere/slab, Go/n alone not whole story
  -- line overlap important or not?
  -- determine thin rates with $\int I(\lambda)\sigma(\lambda)d\lambda$ (no fit)

Summary II

- Line Transfer: -- Optically thick, effectively thin line has higher n_i in sphere vs slab (for same T)
  -- In MC vs ALI beware convergence for $\tau >> 1$
  -- Check levels n_i not just T_R or total I

Photon Processes in (Inhomogeneous) PDRs

Marco Spaans (Kapteyn)

Clumpiness

- Parameter k decreases in expression for R
- For given N_H columns of C+ and C not strongly affected, but spatial extent is
- Column density of CO is boosted in dense clumps
- Back scattering of UV photons causes complicated clump illumination:
  $<\cos\theta>(\lambda)$ and $\omega(\lambda)$
- Influences C+ -> C -> CO transition

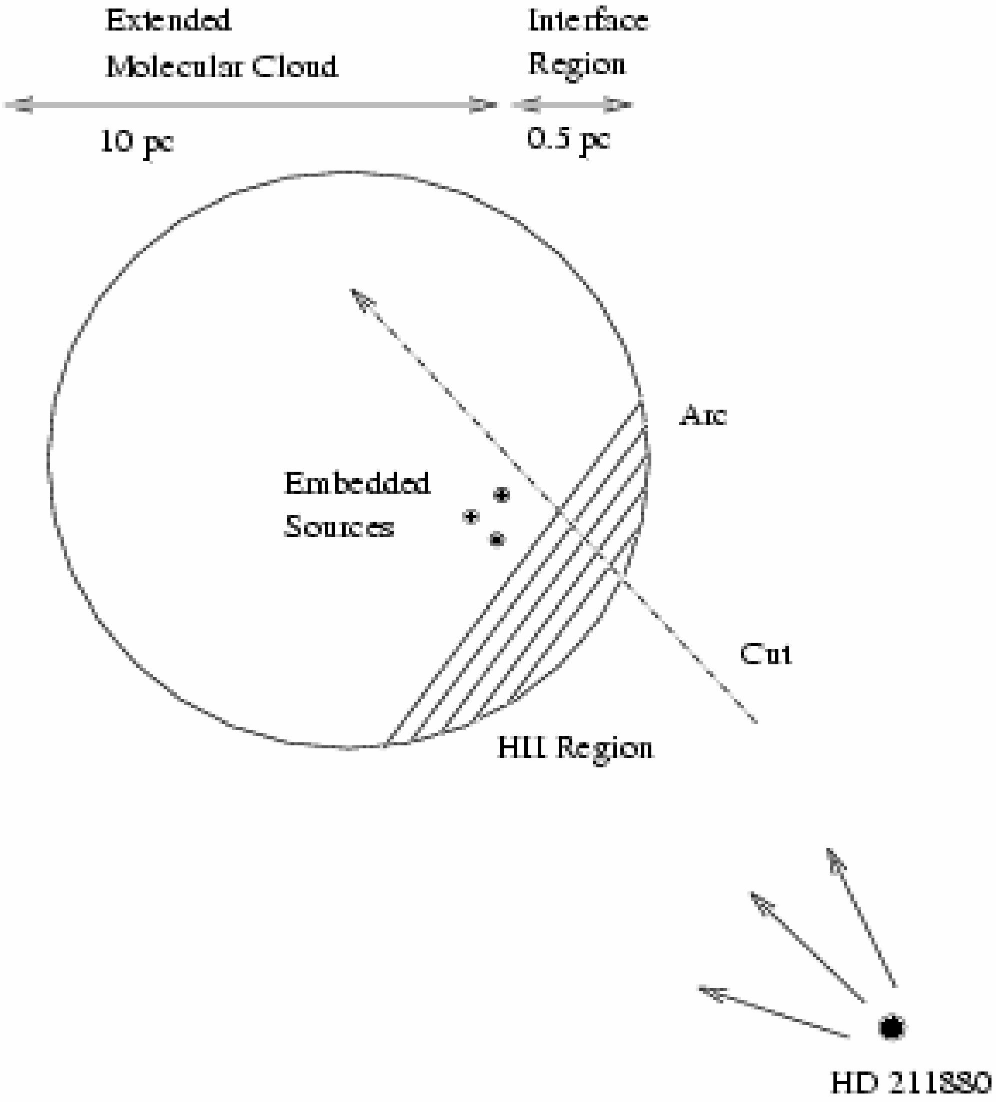

- S140, edge-on PDR
- $n=Fn_c+(1-F)n_i$
- $r=n_c/n_i$, clump size $l_c=0.02$ pc
- Iuv=140, F=30%, r=10, n=2(4) cm-3

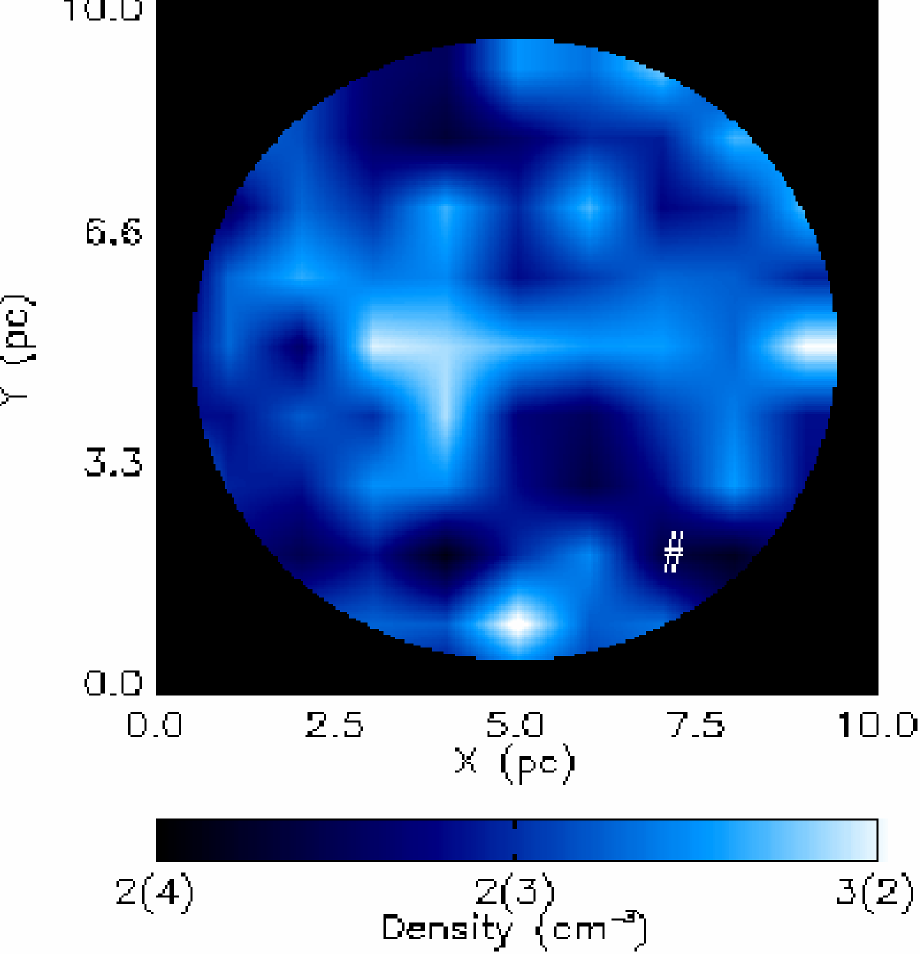

total H density

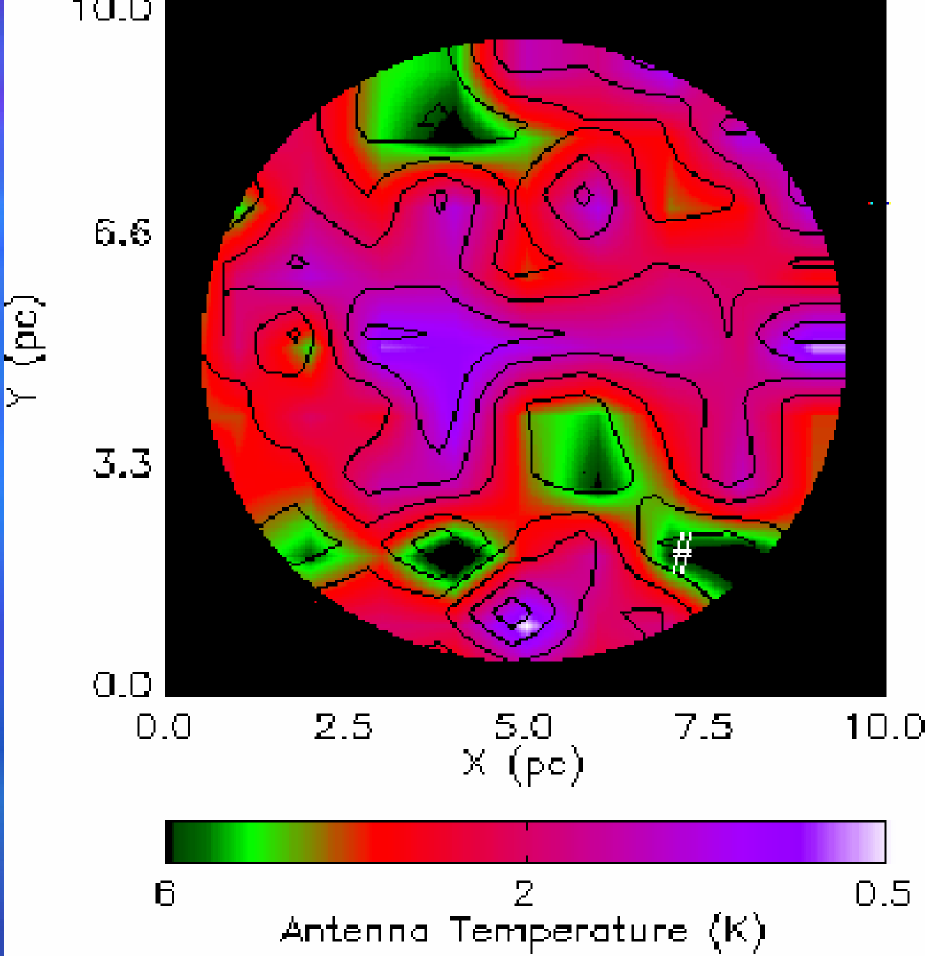

[CI] 609 µm &

^{13}CO 2-1

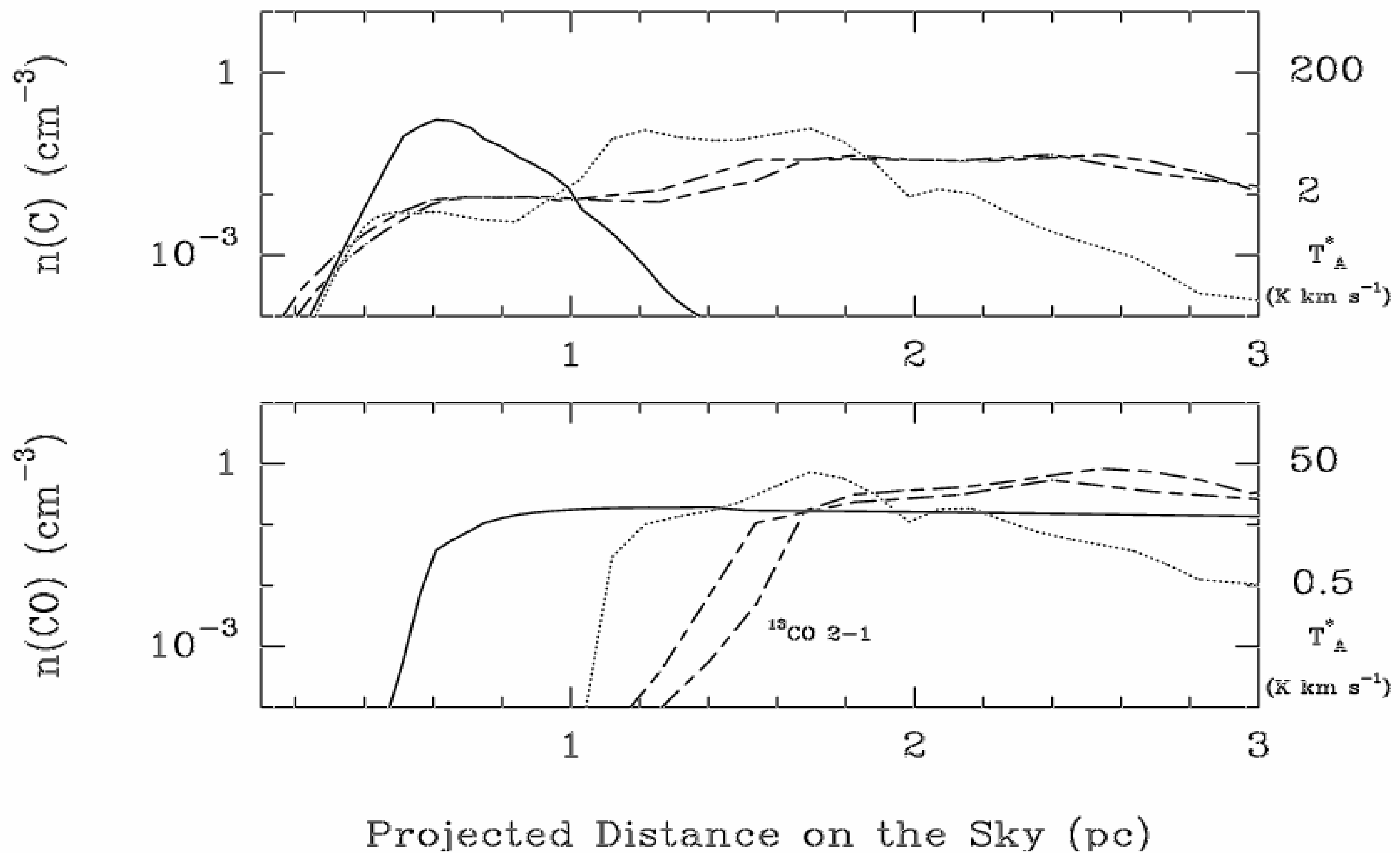
n(C) (cm^{-3})
1
10^{-3}
200
2
T^*_A
(K km s^{-1})
1
2
3
n(CO) (cm^{-3})
1
10^{-3}
50
0.5
T^*_A
(K km s^{-1})
^{13}CO 2−1
1
2
3
Projected Distance on the Sky (pc)

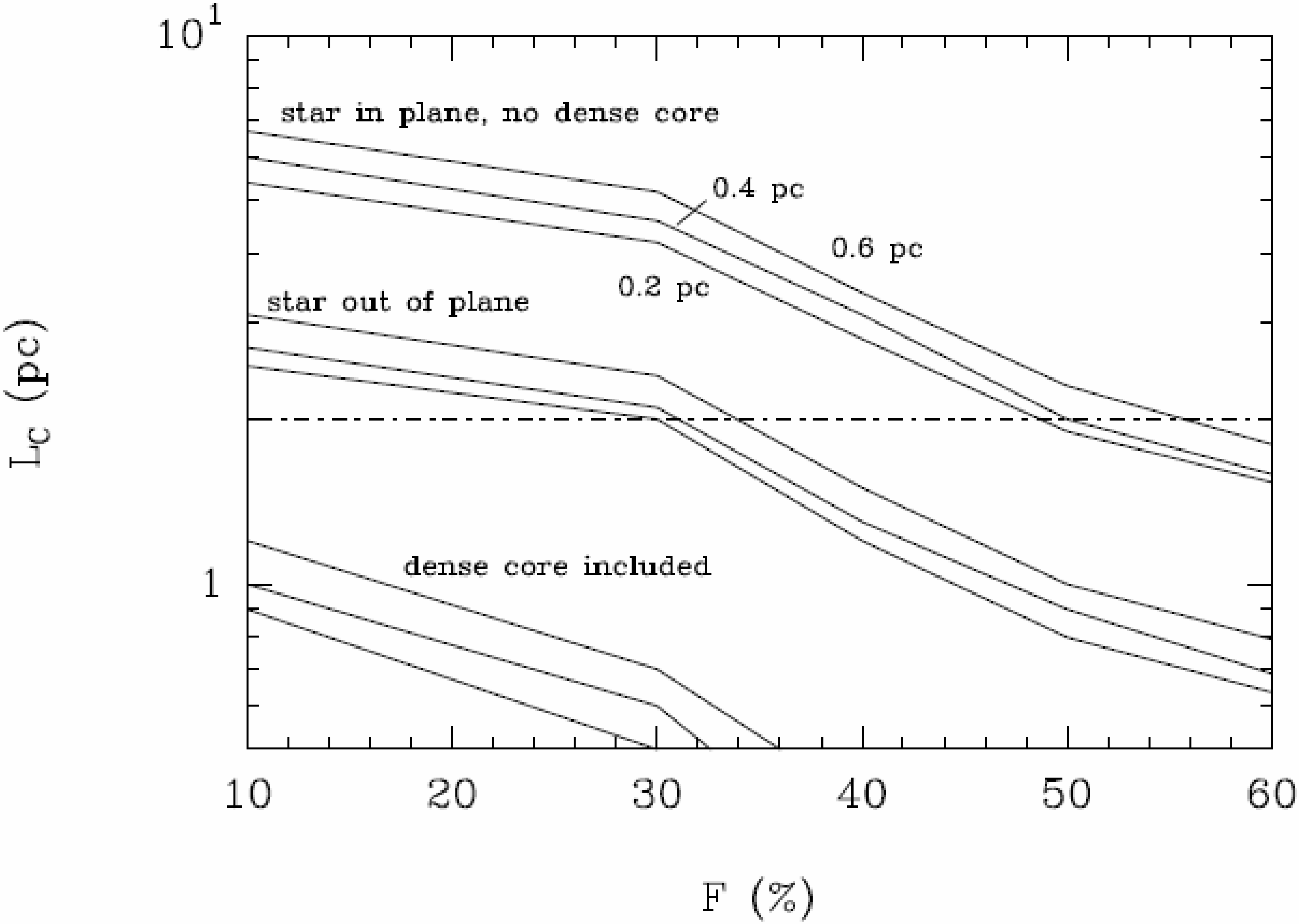
10^1
1
10
20
30
40
50
60
L_C (pc)
F (%)
star in plane, no dense core
0.4 pc
0.6 pc
0.2 pc
star out of plane
dense core included

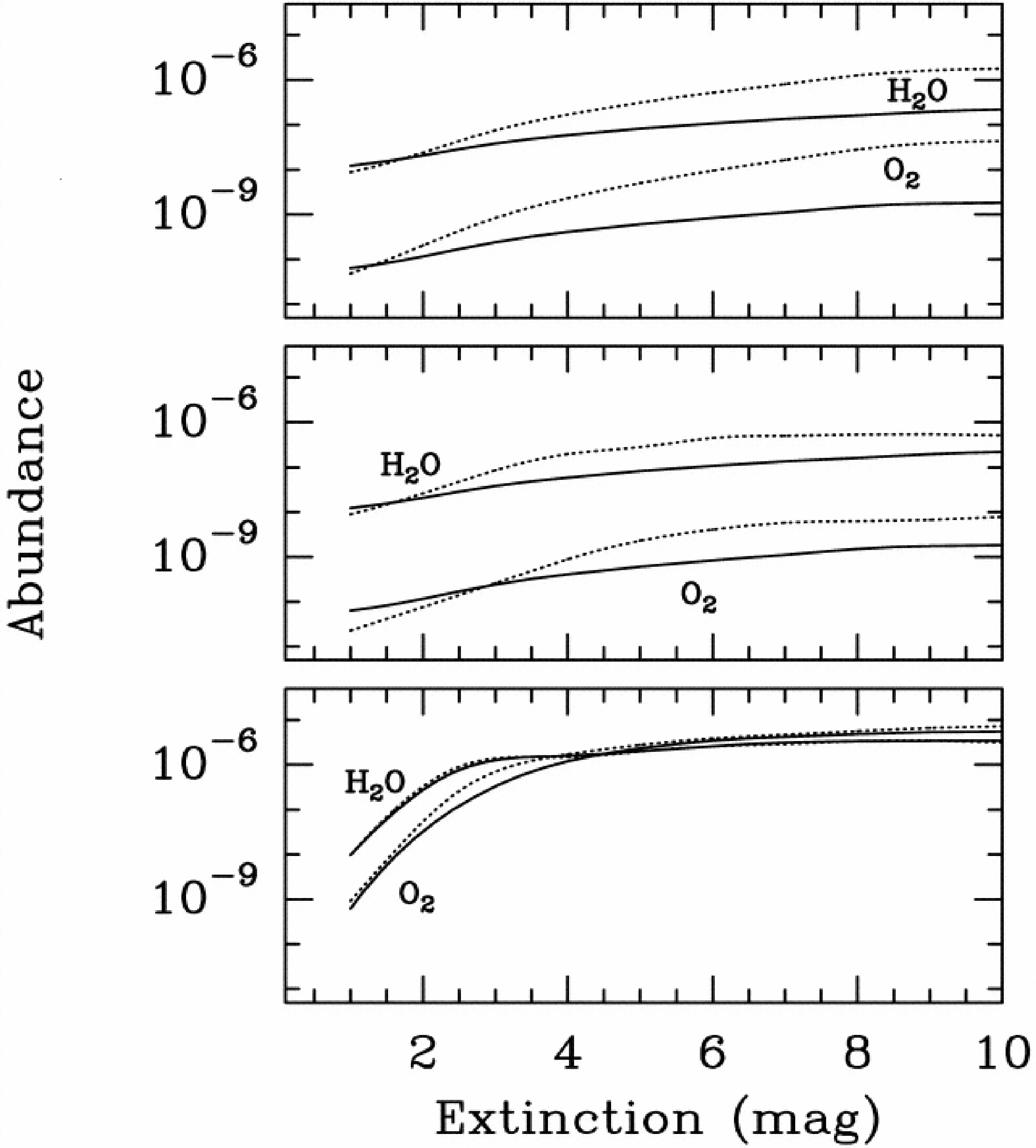
Abundance
10^{-6}
10^{-9}
H_2O
O_2
2
4
6
8
10
Extinction (mag)

H_2 emission

- Fluorescence:
  UV – Vis – IR
  Diagnostic for Iuv/n_H
  No collisional de-excitation if density less than 10^4 cm-3 (same for multiple pumping)
- Scaling: I_F/Iuv (Rn_H/Iuv,N_H) and
  N_H(Rn_H/Iuv,Av)
- Also pure rotational line emission

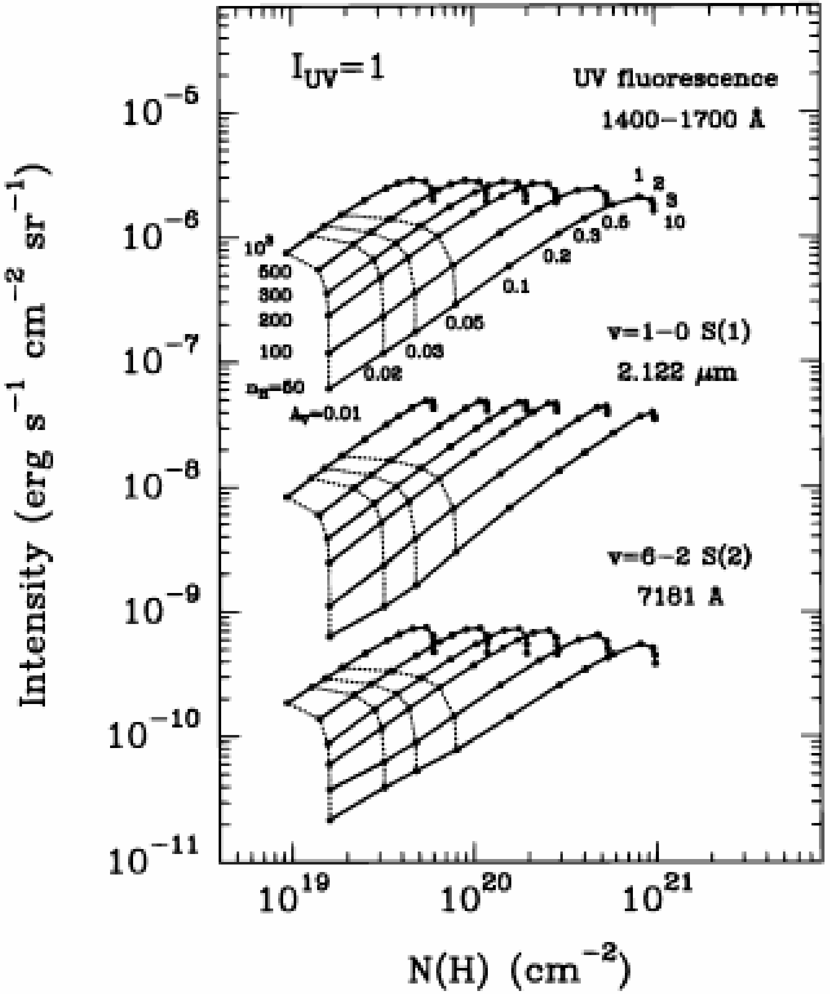
$I_{UV}=1$
UV fluorescence
1400–1700 Å
v=1–0 S(1)
2.122 μm
v=6–2 S(2)
7181 Å
10^3
500
300
200
100
$n_H=50$
$A_V=0.01$
0.02
0.03
0.05
0.1
0.2
0.3
0.5
1
2
3
10
Intensity (erg s^{-1} cm^{-2} sr^{-1})
10^{-5}
10^{-6}
10^{-7}
10^{-8}
10^{-9}
10^{-10}
10^{-11}
10^{19}
10^{20}
10^{21}
N(H) (cm^{-2})

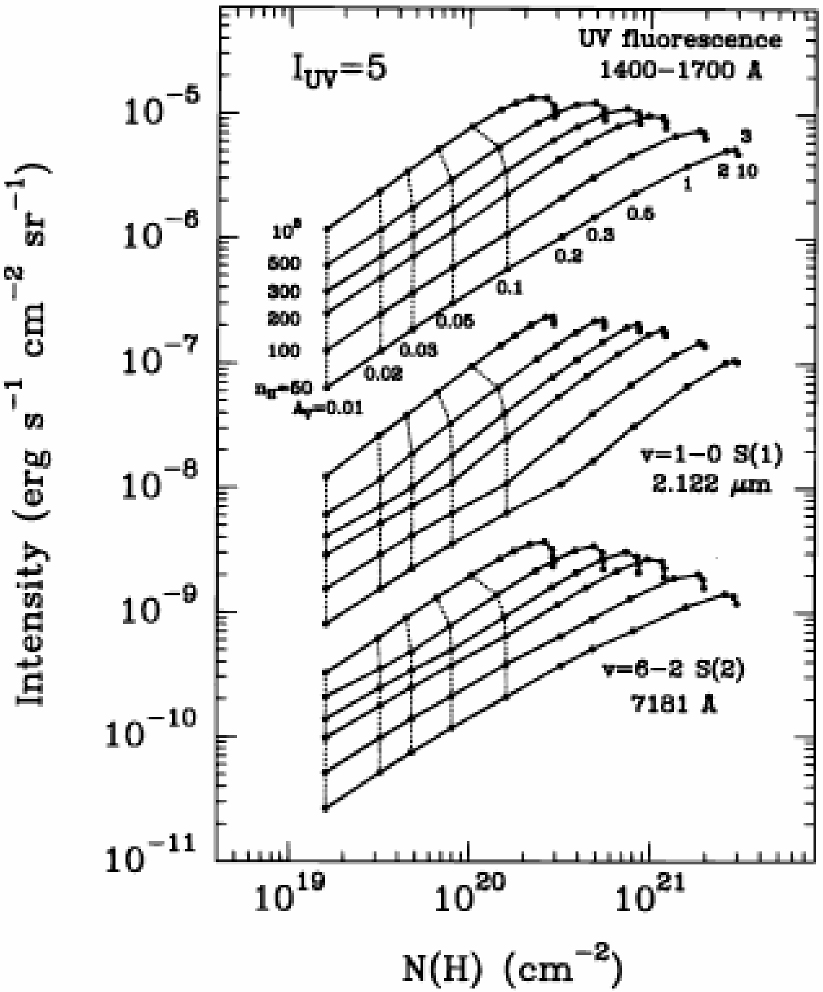
$I_{UV}=5$
UV fluorescence
1400–1700 Å
10^3
500
300
200
100
$n_H=50$
$A_V=0.01$
0.02
0.03
0.05
0.1
0.2
0.3
0.5
1
2
3
10
v=1–0 S(1)
2.122 μm
v=6–2 S(2)
7181 Å
Intensity (erg s^{-1} cm^{-2} sr^{-1})
10^{-5}
10^{-6}
10^{-7}
10^{-8}
10^{-9}
10^{-10}
10^{-11}
10^{19}
10^{20}
10^{21}
N(H) (cm^{-2})

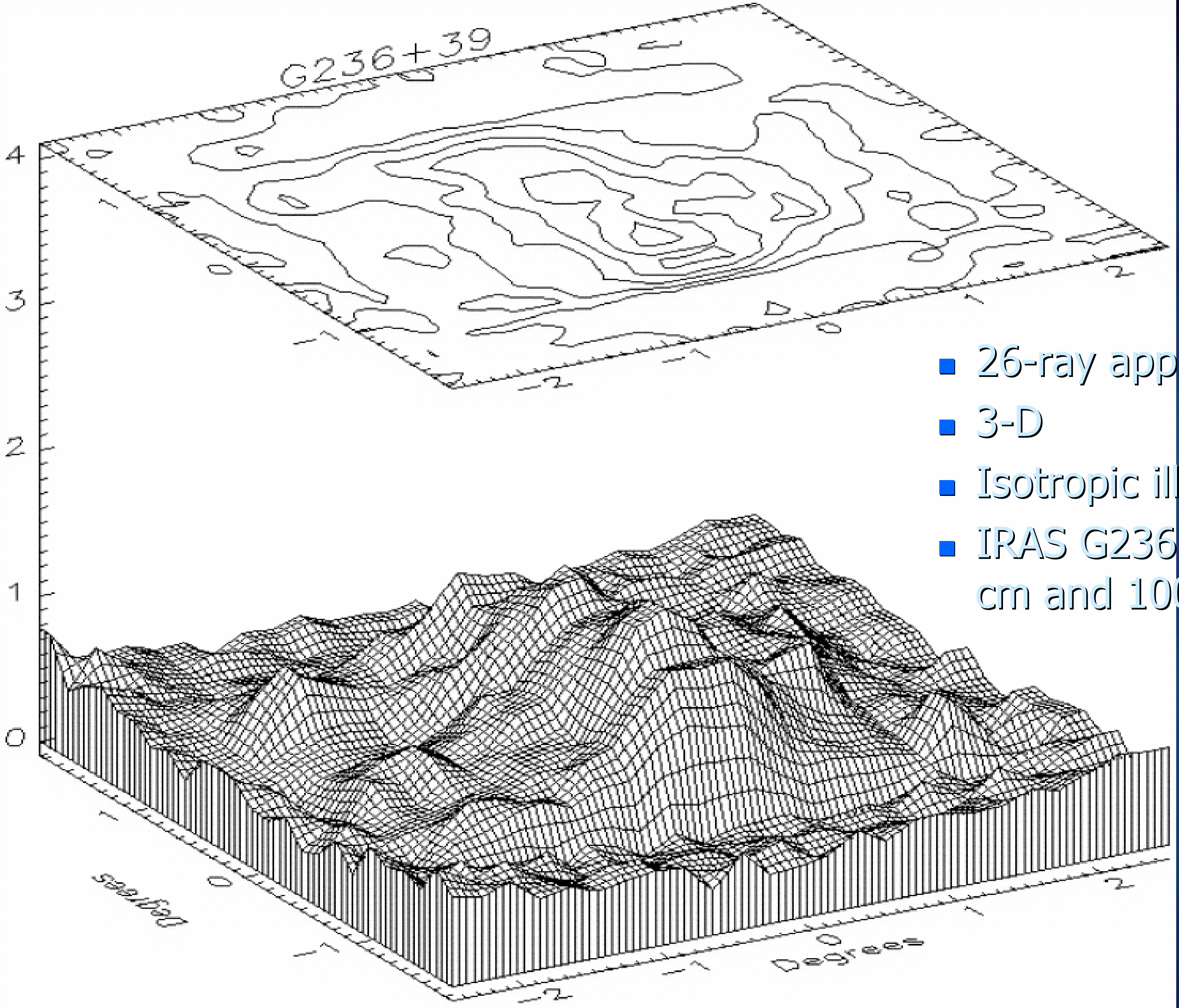

- 26-ray approximation
- 3-D
- Isotropic illumination
- IRAS G236+39: HI 21 cm and 100 μm dust

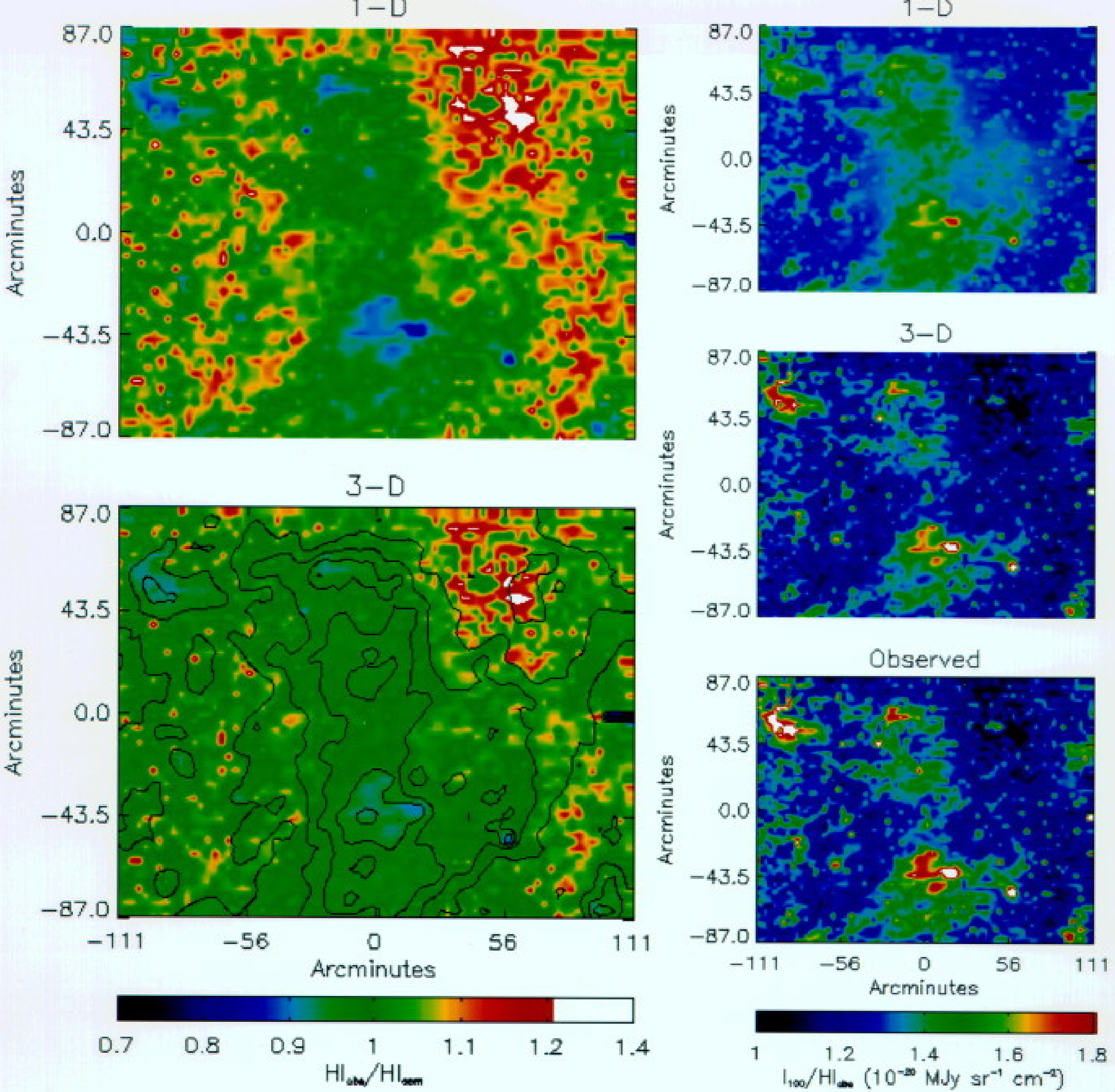

1-D
3-D
1-D
3-D
Observed
87.0
43.5
0.0
−43.5
−87.0
Arcminutes
−111
−56
0
56
111
0.7
0.8
0.9
1
1.1
1.2
1.4
HI_obs/HI_sem
1
1.2
1.4
1.6
1.8
I_100/HI_obs (10^-20 MJy sr^-1 cm^-2)

Photorates with depth

- R=Ro e^(-k Av); Ro strong function of Teff
- k is a fit and k~1-3
- CO (absorptions into pre-dissociated states) and H_2 (Lyman-Werner+cascade) self-shield; TH, de Jong et al.:
  β_{H2}(τ>10)={τ^-1[ln(τ/π^½)]^½+
  (b/τ)^½}erfc(τb/πv^-2)^½
  R_{CO} * [1+αβ_{CO}(τ)]/(1+α) or shielding functions van Dishoeck & Black (1988)

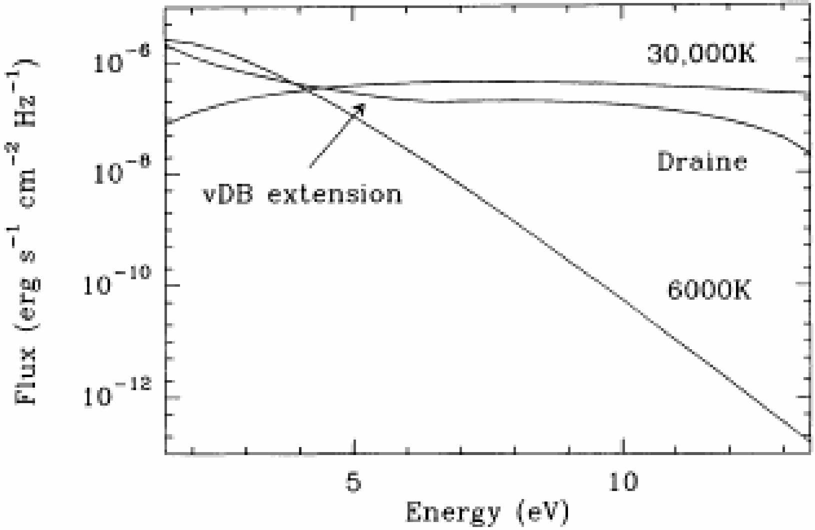

FIG. 2.—Comparison between the Draine (1978) field and the normalized 6000 and 30,000 K blackbody curves. For $\lambda > 2000$ Å, the representation of van Dishoeck & Black (1982) was used.

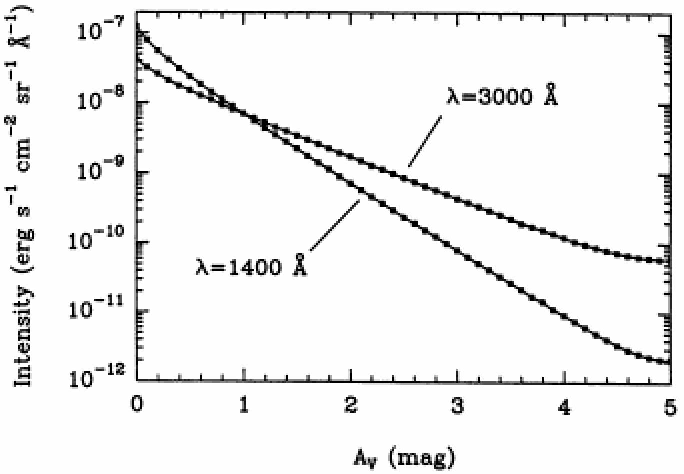

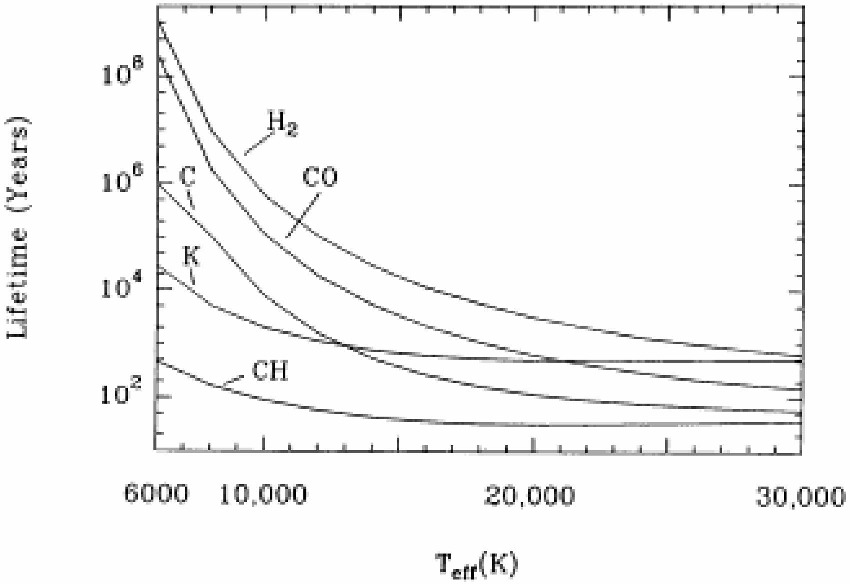

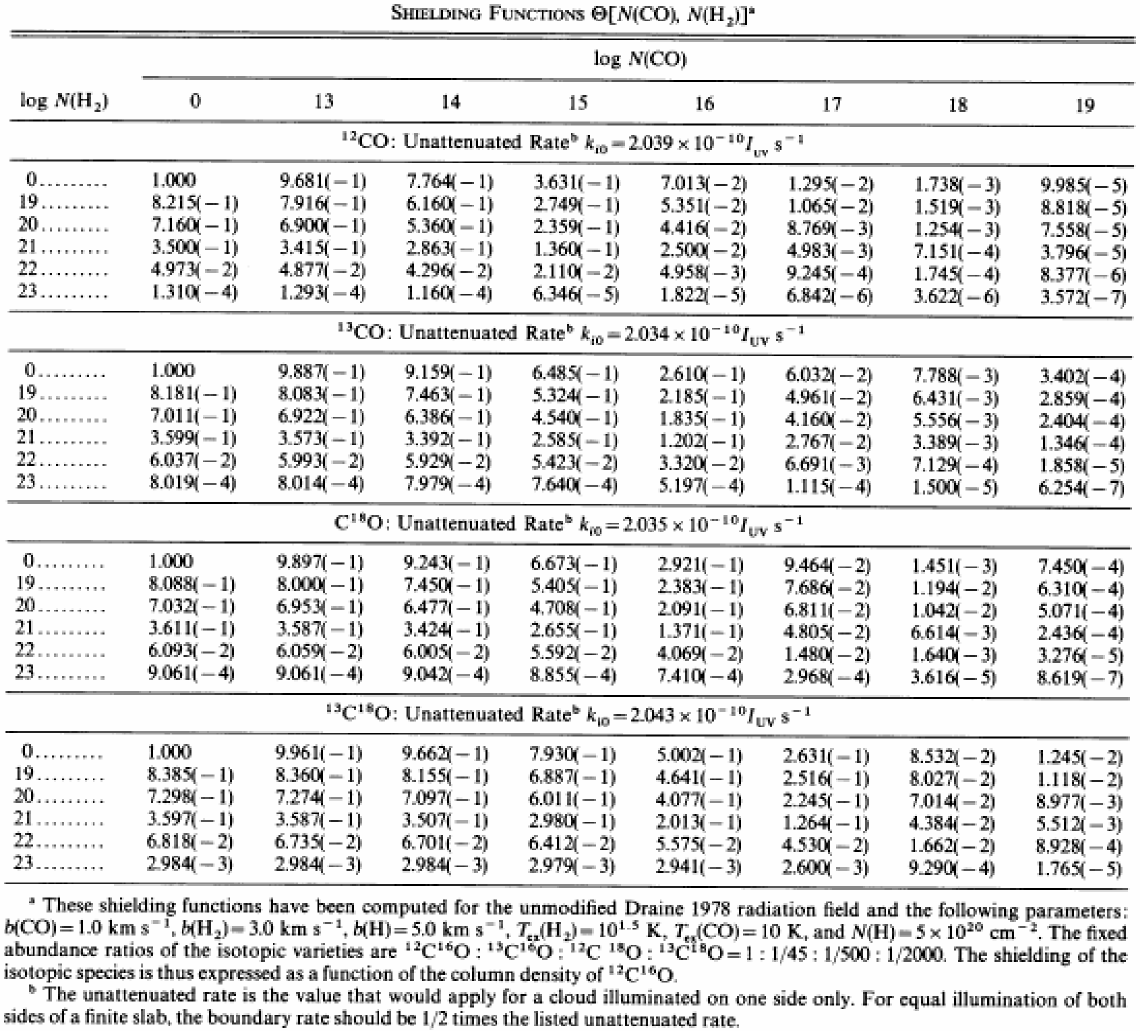

Shielding Functions $\Theta[N(\mathrm{CO}), N(\mathrm{H_2})]$[a]

log $N(H_2)$	log N(CO) 0	13	14	15	16	17	18	19
^{12}CO: Unattenuated Rate[b] $k_{i0} = 2.039 \times 10^{-10} I_{UV}$ s^{-1}								
0………	1.000	9.681(−1)	7.764(−1)	3.631(−1)	7.013(−2)	1.295(−2)	1.738(−3)	9.985(−5)
19………	8.215(−1)	7.916(−1)	6.160(−1)	2.749(−1)	5.351(−2)	1.065(−2)	1.519(−3)	8.818(−5)
20………	7.160(−1)	6.900(−1)	5.360(−1)	2.359(−1)	4.416(−2)	8.769(−3)	1.254(−3)	7.558(−5)
21………	3.500(−1)	3.415(−1)	2.863(−1)	1.360(−1)	2.500(−2)	4.983(−3)	7.151(−4)	3.796(−5)
22………	4.973(−2)	4.877(−2)	4.296(−2)	2.110(−2)	4.958(−3)	9.245(−4)	1.745(−4)	8.377(−6)
23………	1.310(−4)	1.293(−4)	1.160(−4)	6.346(−5)	1.822(−5)	6.842(−6)	3.622(−6)	3.572(−7)
^{13}CO: Unattenuated Rate[b] $k_{i0} = 2.034 \times 10^{-10} I_{UV}$ s^{-1}								
0………	1.000	9.887(−1)	9.159(−1)	6.485(−1)	2.610(−1)	6.032(−2)	7.788(−3)	3.402(−4)
19………	8.181(−1)	8.083(−1)	7.463(−1)	5.324(−1)	2.185(−1)	4.961(−2)	6.431(−3)	2.859(−4)
20………	7.011(−1)	6.922(−1)	6.386(−1)	4.540(−1)	1.835(−1)	4.160(−2)	5.556(−3)	2.404(−4)
21………	3.599(−1)	3.573(−1)	3.392(−1)	2.585(−1)	1.202(−1)	2.767(−2)	3.389(−3)	1.346(−4)
22………	6.037(−2)	5.993(−2)	5.929(−2)	5.423(−2)	3.320(−2)	6.691(−3)	7.129(−4)	1.858(−5)
23………	8.019(−4)	8.014(−4)	7.979(−4)	7.640(−4)	5.197(−4)	1.115(−4)	1.500(−5)	6.254(−7)
C^{18}O: Unattenuated Rate[b] $k_{i0} = 2.035 \times 10^{-10} I_{UV}$ s^{-1}								
0………	1.000	9.897(−1)	9.243(−1)	6.673(−1)	2.921(−1)	9.464(−2)	1.451(−3)	7.450(−4)
19………	8.088(−1)	8.000(−1)	7.450(−1)	5.405(−1)	2.383(−1)	7.686(−2)	1.194(−2)	6.310(−4)
20………	7.032(−1)	6.953(−1)	6.477(−1)	4.708(−1)	2.091(−1)	6.811(−2)	1.042(−2)	5.071(−4)
21………	3.611(−1)	3.587(−1)	3.424(−1)	2.655(−1)	1.371(−1)	4.805(−2)	6.614(−3)	2.436(−4)
22………	6.093(−2)	6.059(−2)	6.005(−2)	5.592(−2)	4.069(−2)	1.480(−2)	1.640(−3)	3.276(−5)
23………	9.061(−4)	9.061(−4)	9.042(−4)	8.855(−4)	7.410(−4)	2.968(−4)	3.616(−5)	8.619(−7)
^{13}C^{18}O: Unattenuated Rate[b] $k_{i0} = 2.043 \times 10^{-10} I_{UV}$ s^{-1}								
0………	1.000	9.961(−1)	9.662(−1)	7.930(−1)	5.002(−1)	2.631(−1)	8.532(−2)	1.245(−2)
19………	8.385(−1)	8.360(−1)	8.155(−1)	6.887(−1)	4.641(−1)	2.516(−1)	8.027(−2)	1.118(−2)
20………	7.298(−1)	7.274(−1)	7.097(−1)	6.011(−1)	4.077(−1)	2.245(−1)	7.014(−2)	8.977(−3)
21………	3.597(−1)	3.587(−1)	3.507(−1)	2.980(−1)	2.013(−1)	1.264(−1)	4.384(−2)	5.512(−3)
22………	6.818(−2)	6.735(−2)	6.701(−2)	6.412(−2)	5.575(−2)	4.530(−2)	1.662(−2)	8.928(−4)
23………	2.984(−3)	2.984(−3)	2.984(−3)	2.979(−3)	2.941(−3)	2.600(−3)	9.290(−4)	1.765(−5)

[a] These shielding functions have been computed for the unmodified Draine 1978 radiation field and the following parameters: $b(\mathrm{CO}) = 1.0$ km s^{-1}, $b(\mathrm{H_2}) = 3.0$ km s^{-1}, $b(\mathrm{H}) = 5.0$ km s^{-1}, $T_{ex}(\mathrm{H_2}) = 10^{1.5}$ K, $T_{ex}(\mathrm{CO}) = 10$ K, and $N(\mathrm{H}) = 5 \times 10^{20}$ cm^{-2}. The fixed abundance ratios of the isotopic varieties are $^{12}C^{16}O : {}^{13}C^{16}O : {}^{12}C^{18}O : {}^{13}C^{18}O = 1 : 1/45 : 1/500 : 1/2000$. The shielding of the isotopic species is thus expressed as a function of the column density of $^{12}C^{16}O$.

[b] The unattenuated rate is the value that would apply for a cloud illuminated on one side only. For equal illumination of both sides of a finite slab, the boundary rate should be 1/2 times the listed unattenuated rate.

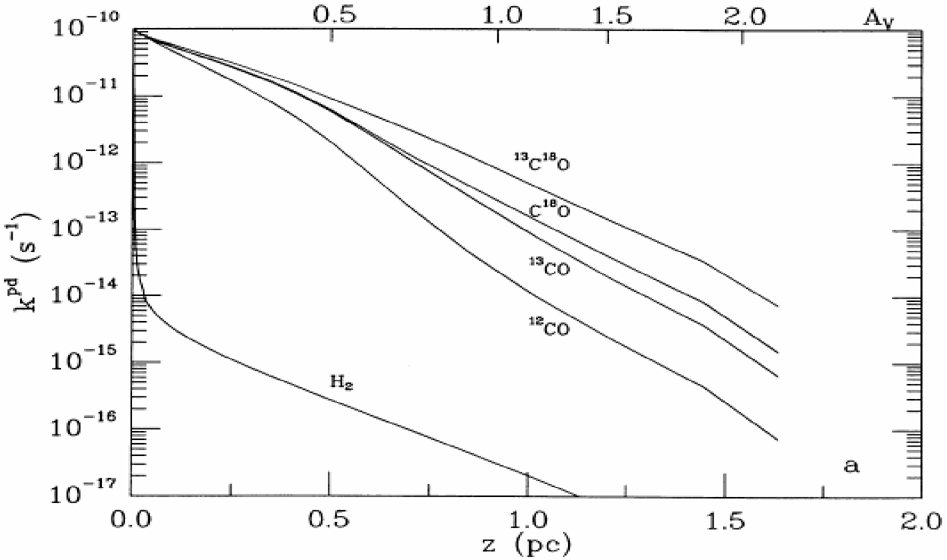

FIG. 5*a*

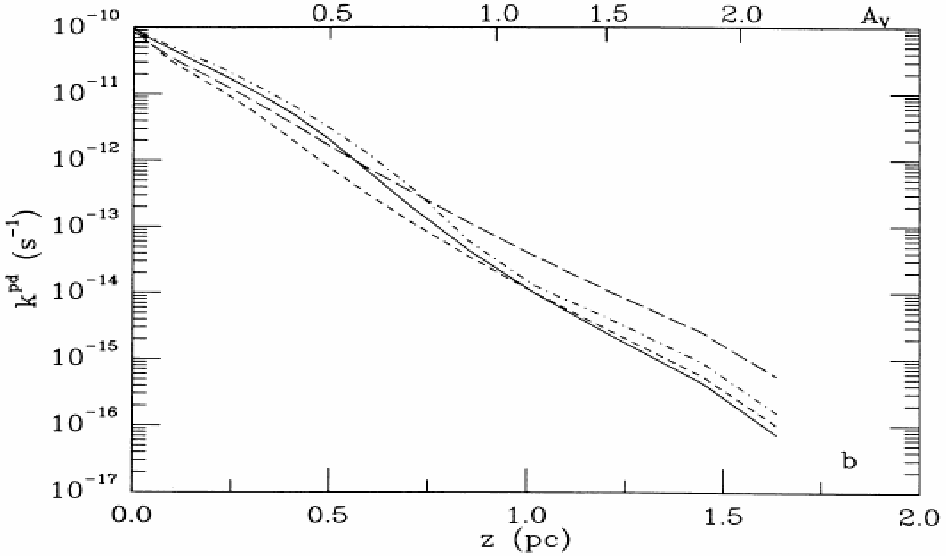

FIG. 5*b*

FIG. 5.—(*a*) Photodissociation rates of ^{12}CO and the isotopic varieties as functions of linear depth into translucent cloud model T6. See Table 7 for details of the model. (*b*) Photodissociation rates of ^{12}CO as functions of linear depth computed at four different levels of approximation. *Solid curve:* full calculation including self-shielding, mutual shielding, shielding by lines of H and H_2 and dust attenuation for all CO lines up to $J'' = 9$. *Short-dashed curve:* calculation including only the *R*(0) lines of CO and H_2 lines with $J'' = 0$ and 1. *Long-dashed line:* calculation in which only self-shielding in the CO *R*(0) lines and dust attenuation is taken into account. *Dash-dotted line:* calculation using the shielding functions presented in Table 5.

Photorates with depth

- Good if line overlap is ignored; edge effects still occur; Iuv/n_H ratio crucial
- H_2* (v=6/2.6 eV) versus H_2 (J,v)
- Line overlap: H_2 , H, CO, C
- MC H_2: N=135, λ=1000 Å, f=3.5(-3), A=5.7(8) s-1, η=0.127
- MC CO: N=33, λ=1002 Å, f=2.0(-2), A=3.0(11), η=1.0

Photorates with depth

- Should integrate photo-ionization and photo-dissociation cross sections: $\sigma(\lambda)$
- Note: CRs and X-rays can be important;

  CRs no attenuation, X-rays column of N_H~10^22 cm-2

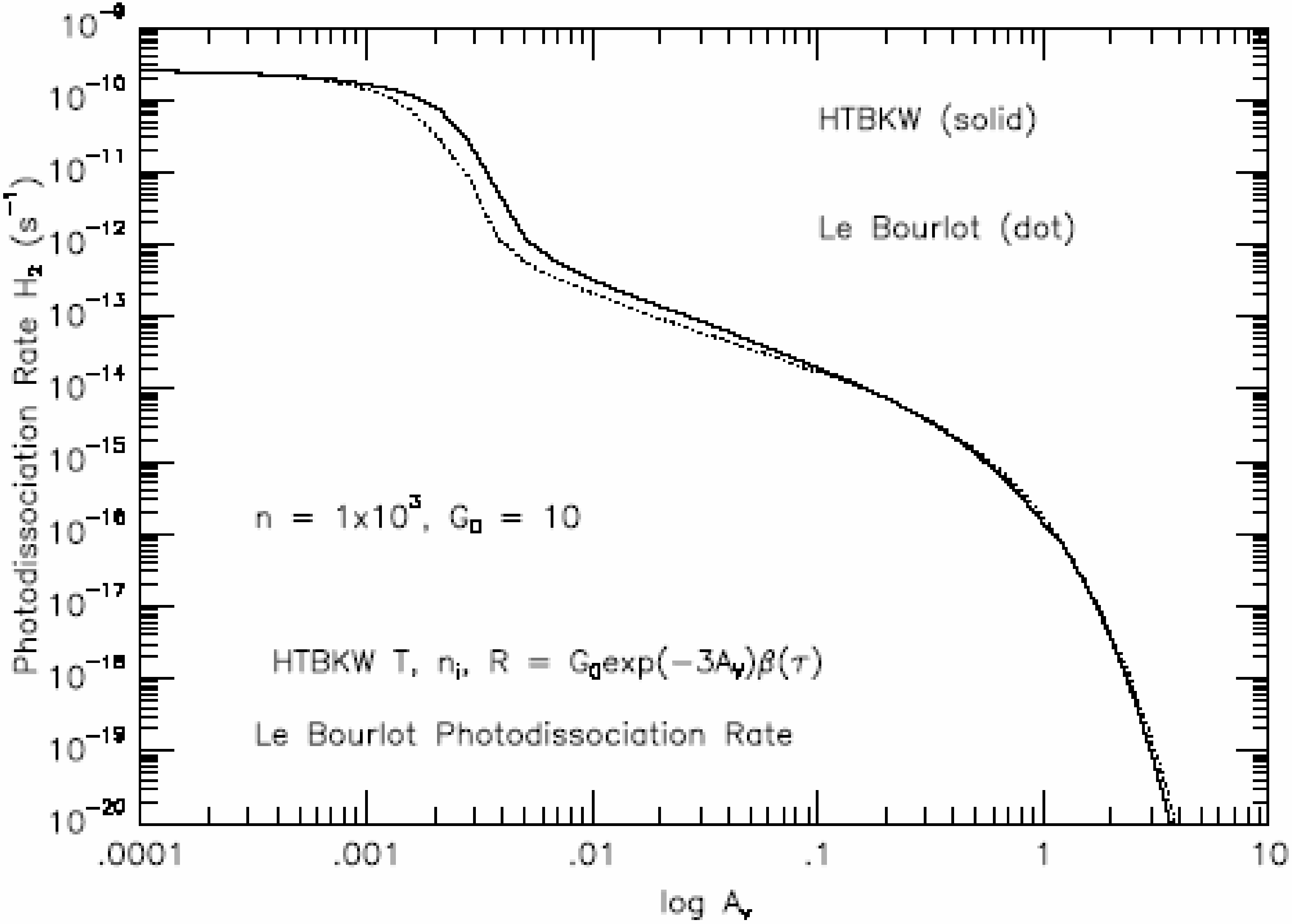
HTBKW (solid)
Le Bourlot (dot)
n = 1x10^3, G_0 = 10
HTBKW T, n_i, R = $G_0 \exp(-3A_V)\beta(\tau)$
Le Bourlot Photodissociation Rate
Photodissociation Rate H_2 (s^{-1})
10^{-9}
10^{-10}
10^{-11}
10^{-12}
10^{-13}
10^{-14}
10^{-15}
10^{-16}
10^{-17}
10^{-18}
10^{-19}
10^{-20}
.0001
.001
.01
.1
1
10
log A_V

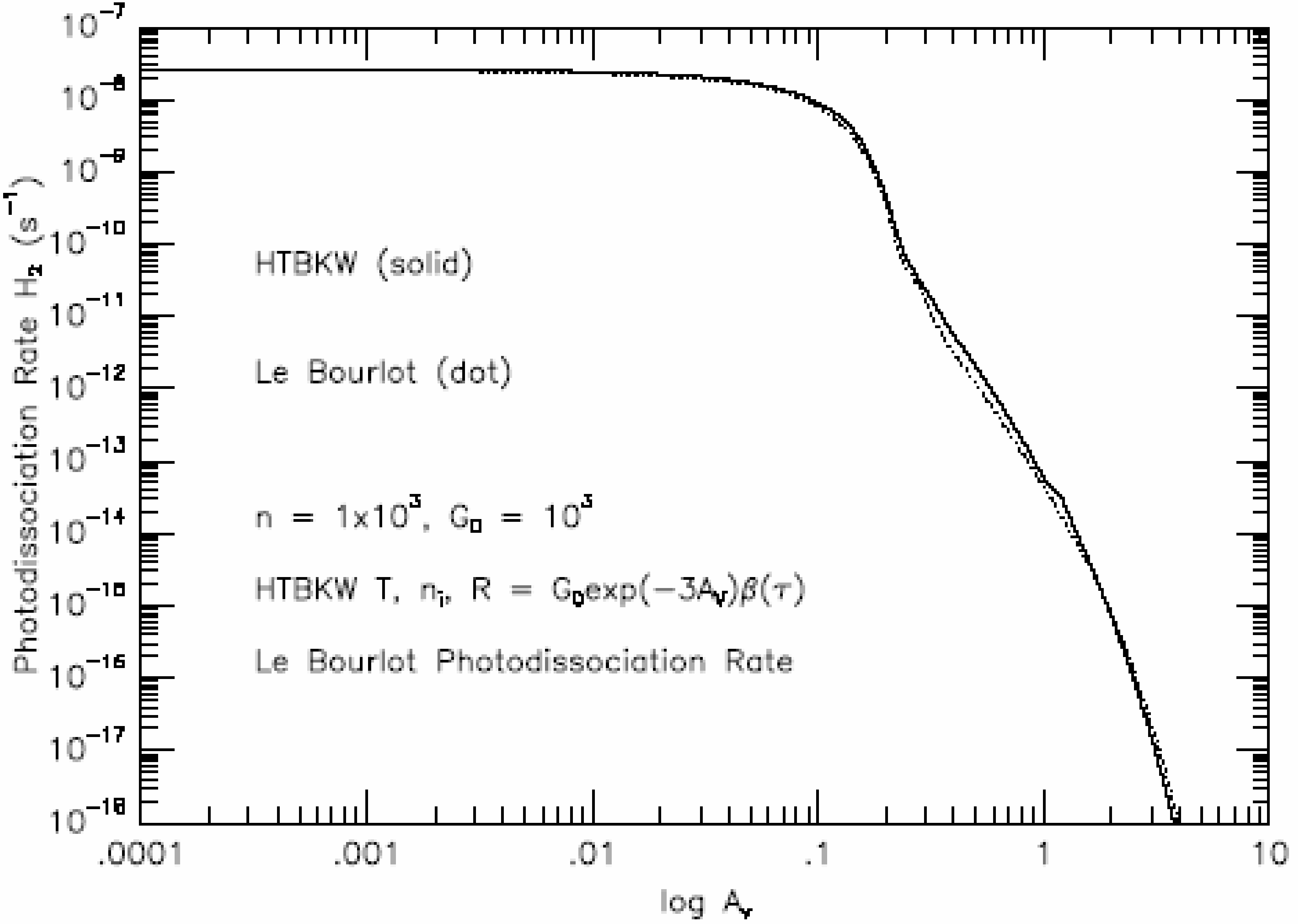
HTBKW (solid)
Le Bourlot (dot)
$n = 1 \times 10^3$, $G_0 = 10^3$
HTBKW T, n_i, $R = G_0 \exp(-3A_V)\beta(\tau)$
Le Bourlot Photodissociation Rate
Photodissociation Rate H_2 (s^{-1})
log A_V
10^{-7}
10^{-8}
10^{-9}
10^{-10}
10^{-11}
10^{-12}
10^{-13}
10^{-14}
10^{-15}
10^{-16}
10^{-17}
10^{-18}
.0001
.001
.01
.1
1
10

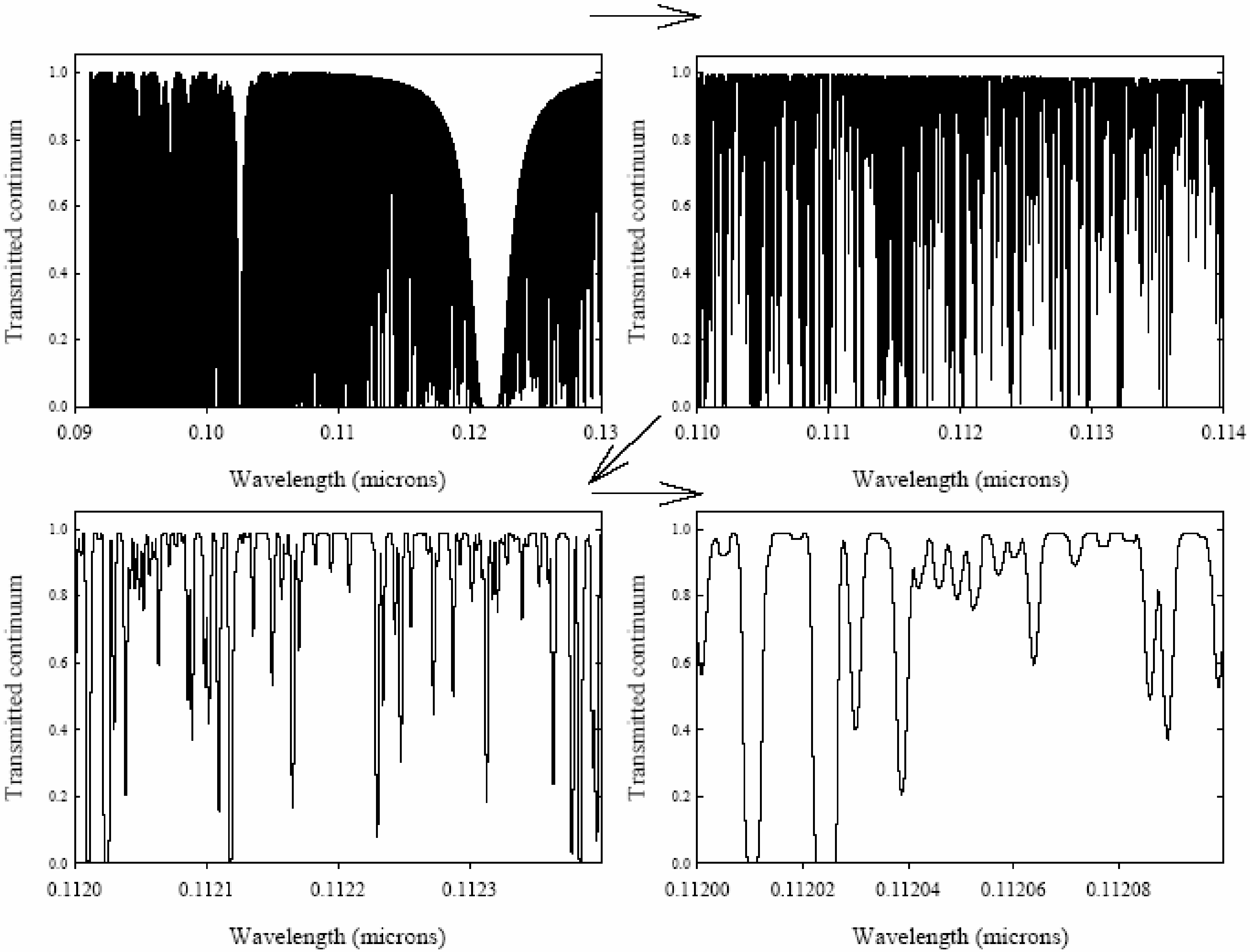
Transmitted continuum
1.0
0.8
0.6
0.4
0.2
0.0
0.09
0.10
0.11
0.12
0.13
Wavelength (microns)
Transmitted continuum
1.0
0.8
0.6
0.4
0.2
0.0
0.110
0.111
0.112
0.113
0.114
Wavelength (microns)
Transmitted continuum
1.0
0.8
0.6
0.4
0.2
0.0
0.1120
0.1121
0.1122
0.1123
Wavelength (microns)
Transmitted continuum
1.0
0.8
0.6
0.4
0.2
0.0
0.11200
0.11202
0.11204
0.11206
0.11208
Wavelength (microns)

TABLE 2

PHOTOIONIZATION AND DISSOCIATION RATES FOR DIFFERENT BLACKBODY RADIATION FIELDS WITH $G_0 = 1$

	T_{eff} in K													
	6000		8000		10,000		14,000		18,000		24,000		30,000	
Reaction	a	b	a	b	a	b	a	b	a	b	a	b	a	b
$C \rightarrow C^+ + e^-$	2.82(-15)	3.27	2.70(-13)	3.30	3.50(-12)	3.33	4.92(-11)	3.36	1.63(-10)	3.38	3.42(-10)	3.39	4.50(-10)	3.40
$CH^{+\dagger} \rightarrow C + H^+$	3.86(-13)	1.35	1.17(-12)	1.41	3.24(-12)	1.59	2.12(-11)	2.02	6.90(-11)	2.31	1.62(-10)	2.57	2.36(-10)	2.71
$OH \rightarrow O + H$	6.66(-13)	1.81	7.70(-12)	1.90	3.12(-11)	1.94	1.28(-10)	2.00	2.30(-10)	2.05	3.00(-10)	2.10	3.08(-10)	2.14
$CH \rightarrow C + H$	8.30(-11)	1.32	2.10(-10)	1.37	3.60(-10)	1.43	6.62(-10)	1.56	8.32(-10)	1.65	8.20(-10)	1.74	7.18(-10)	1.78
$CH \rightarrow CH^+ + e^-$	8.12(-15)	3.10	7.08(-13)	3.16	8.80(-12)	3.20	1.19(-10)	3.25	3.88(-10)	3.28	8.02(-10)	3.39	1.05(-9)	3.32
$H_2O \rightarrow OH + H$	1.65(-12)	1.84	1.92(-11)	1.86	7.28(-11)	1.89	2.76(-10)	1.94	4.78(-10)	1.99	6.14(-10)	2.05	6.30(-10)	2.10
$CH_2 \rightarrow CH + H$	1.15(-11)	2.00	8.78(-11)	1.99	2.50(-10)	1.98	6.42(-10)	1.98	8.56(-10)	1.98	8.42(-10)	2.00	7.32(-10)	2.01
$Mg \rightarrow Mg^+ + e^-$	1.66(-11)	1.95	2.48(-12)	1.96	1.05(-11)	1.98	4.16(-11)	2.00	7.92(-11)	2.01	8.06(-11)	2.03	7.58(-11)	2.04
$SiO \rightarrow Si + O$	1.62(-13)	2.17	3.62(-12)	2.18	1.94(-11)	2.19	9.90(-11)	2.21	1.87(-10)	2.22	2.42(-10)	2.23	2.40(-10)	2.24
$Fe \rightarrow Fe^+ + e^-$	2.12(-13)	2.08	4.30(-12)	2.12	2.24(-11)	2.14	1.13(-10)	2.17	2.12(-10)	2.19	2.74(-10)	2.21	2.72(-10)	2.22
$S \rightarrow S^+ + e^-$	1.20(-14)	2.78	7.50(-13)	2.84	7.64(-12)	2.89	9.10(-11)	2.95	2.80(-10)	3.00	5.58(-10)	3.05	7.20(-10)	3.07
$O_2 \rightarrow O + O$	1.13(-12)	1.98	1.86(-11)	2.01	8.46(-11)	2.03	3.64(-10)	2.06	6.40(-10)	2.08	7.88(-10)	2.10	7.72(-10)	2.12
$Si \rightarrow Si^+ + e^-$	1.77(-12)	2.13	3.80(-11)	2.15	2.40(-10)	2.17	1.07(-9)	2.21	2.10(-9)	2.23	2.84(-9)	2.26	2.92(-9)	2.27
$H_2^+ \rightarrow H + H^+$	3.78(-13)	1.95	5.40(-12)	2.01	2.84(-11)	2.07	1.49(-10)	2.16	3.08(-10)	2.22	4.48(-10)	2.28	4.88(-10)	2.32
$H_2 \rightarrow H + H$	2.02(-17)	2.50	2.72(-15)	2.50	4.48(-14)	2.50	9.25(-13)	2.50	4.55(-12)	2.50	1.68(-11)	2.50	3.41(-11)	2.50
$CO \rightarrow C + O$	9.20(-17)	3.20	1.05(-14)	3.20	1.62(-13)	3.20	3.39(-12)	3.20	1.74(-11)	3.20	7.16(-11)	3.20	1.60(-10)	3.20

NOTES.—The reaction rates are parameterized by a and b according to $R = a \times e^{-bA_V}$, where a is the unattenuated rate. The exponent b reflects only the attenuation due to dust, but not that due to self-shielding or shielding by H_2.

† Notice that this reaction differs from the one given in TH85, Table 5, p.742.

References

- Tielens & Hollenbach 1985
- Kaufman et al. 1999; Spaans 1996; Sternberg & Dalgarno 1995; Stőrzer et al. 1995; Spaans et al. 1994; Wolfire et al. 1993; le Bourlot et al. 1993; Tielens et al. 1993; Boisse’ 1990; van Dishoeck & Black 1988; Sternberg 1988; Black & van Dishoeck 1987; de Jong et al. 1980; Black & Dalgarno 1976
- Maloney et al. 1996